HMM-based Defect Localization in Wire Ropes - A new Approach to Unusual Subsequence Recognition

Esther-Sabrina Platzer[1], Josef Nägele[2], Karl-Heinz Wehking[2] and Joachim Denzler[1]

[1] Chair for Computer Vision, Friedrich Schiller University of Jena
{Esther.Platzer,Joachim.Denzler}@uni-jena.de
http://www.inf-cv.uni-jena.de
[2] Institute of Mechanical Handling and Logistics, University Stuttgart
{Naegele,Karl-Heinz.Wehking}@ift.uni-stuttgart.de
http://www.uni-stuttgart.de/ift

Abstract. Automatic visual inspection has become an important application of pattern recognition, as it supports the human in this demanding and often dangerous work. Nevertheless, often missing abnormal or defective samples prohibit a supervised learning of defect models. For this reason, techniques known as one-class classification and novelty- or unusual event detection have arisen in the past years. This paper presents a new strategy to employ Hidden Markov models for defect localization in wire ropes. It is shown, that the Viterbi scores can be used as indicator for unusual subsequences. This prevents a partition of the signal into sufficient small signal windows at cost of the temporal context. Our results outperform recent time-invariant one-class classification approaches and depict a great advance for an automatic visual inspection of wire ropes.

1 Introduction

Visual inspection of material surfaces has become an important application of pattern recognition [1–4]. Especially in scenarios, in which a manual inspection implies a high risk for the human life an automatic inspection is highly appreciated. Furthermore, in case of long-time inspections a human suffers from fatigue and a reduced level of concentration. The inspection of wire ropes of ropeways, elevators or bridges is an example for such a dangerous and at the same time demanding inspection task. As the ropes cannot be unmounted, a manual inspection bears a high risk for the human life. The inspection speed is often quite high (0.5 meters/s) and defects are small and nearly invisible. In Fig. 1(a) two

This manuscript is originally published in *Pattern Recognition, Lecture Notes in Computer Science, Volume 5748, Springer, 2009, pp 442–451.*
The final publication is available at
http://link.springer.com/chapter/10.1007%2F978-3-642-03798-6_45

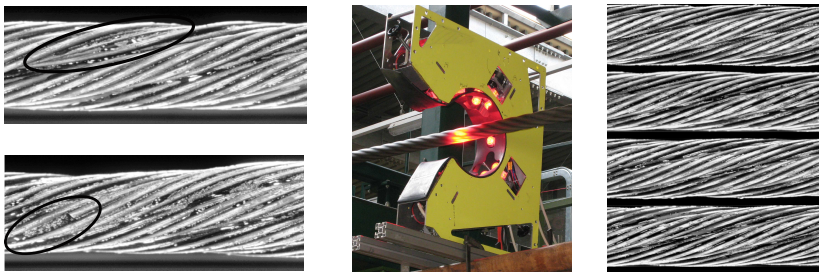

(a) Rope defects (b) Prototype system (c) Rope views

Fig. 1. (a) Two common kind of rope defects: a missing wire (top) and a wire fraction (bottom). (b) the prototype system leading to four different rope views (c).

common classes of surface defects in wire ropes are shown: a missing wire and a wire fraction. In order to afford an automatic visual inspection of wire ropes, a prototype system displayed in Fig. 1(b) was developed [5]. Line cameras project the rope to a fixed number of rope views, visible in Fig. 1(c).
As it becomes clear from Fig. 1(a) surface defects in wire ropes are not obvious. Therefore, a machine-based recognition is a challenging problem. Furthermore, a frequently reported problem in automatic visual inspection is the lack of faulty, abnormal examples. It is hard to obtain defective examples from a real ropeway, especially due to the strict rules for a regular visual examination [6]. In order to cope with the missing abnormal training material, one-class classification approaches, also known as novelty detection or unusual event detection, have arisen the past years [7, 1, 3, 4, 8].

A brief overview of visual inspection and one-class classification is given in the following section. In Sect. 3 anomaly detection with Hidden-Markov models is introduced, followed by a derivation of our new strategy for the detection of anomalous subsequences. The ratio between the maximum Viterbi scores of two consecutive time steps serves as anomaly indicator and the theoretical meaning of this ratio is derived. In Sect. 5 the method and the payoff are summarized and discussed followed by an outlook on future work.

2 Related Work

One-class classification (OCC) [7] is a concept often used in automatic visual inspection applications. The key idea is to learn only a representation of a target class - mostly the class of intact examples. Afterwards, anomalies and defects are recognized by outlier detection. Xie [4] provides a comprehensive summary of recent advances in visual inspection coping also with one-class classification strategies for anomaly and defect detection. In [9] and [10] general novelty and outlier detection methods are subsumed. Application examples in the field of automatic visual inspection are given by Maenpaa et al. [1], who use self-organizing

Fig. 2. Result of the automatic defect detection in wire ropes presented in [8]. The white window borders the rope region, which was classified as potential defect.

maps for real-time surface inspection. Xie and Mirmehdi [11, 3] employ a Gaussian mixture model (GMM) to detect abnormal variations from the random texture of ceramic tiles. In [12] an OCC approach using a GMM for automatic defect detection in wire ropes is presented. Potential defects in ropes are identified by an outlier detection scheme. The work is extended in [8] by a comparison of different features. The approach allows a defect detection in wire ropes, but its localization ability is strongly restricted. Fig. 2 shows an exemplary detection result obtained with our implementation of the approach of Platzer et al. [8]. Obviously, just a small part of the defect was recovered. Our working hypothesis states, that defect detection and localization can be improved by the usage of temporal context during the classification.

Hidden Markov models (HMM) are a well-known technique to incorporate temporal context from time series into classification problems. OCC in the context of sequential instead of static data is often called unusual event detection. For example, Zhang et al. [13] present a semi-supervised HMM approach for unusual event detection. A HMM explaining usual events is learned from a huge amount of normal training data. Unusual events are recognized by a reduced likelihood of the data given the model, and the model is adapted to this unusual events by a Bayesian approach. Brewer et al. [14] employ coupled Hidden Markov models (CHMM) to identify suspects in digital forensics. An application to surface inspection based on CHMMs is presented by Pernkopf [2]. A defect localization in texture using HMMs was presented by Hadizadeh and Shokouhi [15]. They utilize the HMM as a texture unit descriptor and predict the pixel values of the texture. Defect detection is performed, based on the prediction error.

In most HMM-based anomaly detection approaches a decision is made based on the sequence likelihood given the learned model. By windowing the signal it is possible to get a better localization, but at the expense of less temporal context. So, obviously these are opposing intentions. For our purpose, a preferably wide temporal context covering at least one rope period is important. At the same time, an exact localization of defects within the sequence would be a great improvement. Therefore, in the following section HMM-based anomaly detection will be explained more detailed and a new approach for the recognition of unusual subsequences will be introduced.

3 HMM-based Anomaly Detection

A Hidden Markov model is a probabilistic graphical model for a two-step random process. In the context of wire rope surface analysis the rope views are treated as observation sequences, whereas the hidden states are linked to the position in the rope. Emission distributions are modeled by a GMM based on histograms of oriented gradients (HOG) [16], which serve as features. This feature choice is motivated by the regular rope structure ruled by gradients oriented perpendicular to the twist direction. To improve the discrimination ability of features, also the entropy of each HOG cell is computed and used within the features. As it is no problem to obtain a lot of intact rope data, model learning is performed in the usual way by the well-known Baum-Welch algorithm [17]. Due to the periodic structure of wire ropes, a cyclic model with a fixed bandwidth is used preventing an error-prone segmentation of the training data into periodic segments. By defining a threshold on the probability of the observation sequence given the model a decision of the sequence belonging to the model can be made. Again it should be referred to the opposing goals: by separating the signal into effectual small test sequences it is possible to achieve a good localization, but at cost of the temporal context used to compare the test sequence with the model. For this reason, the following section introduces a new way for an HMM-based recognition of unusual subsequences.

3.1 Unusual Subsequence Detection

To decode the optimal state sequence given a learned HMM λ and an observation sequence $\boldsymbol{O}_{1:T}$ of length T, the Viterbi algorithm is used [17]. Based on the Viterbi score $\delta_t(i) = \max_{S_1,\ldots,S_{t-1}} P(S_1,\ldots,S_t = s_i, o_1,\ldots,o_t \mid \lambda)$ at time t for state $S_t = s_i$, the likelihood of the optimal path (marked by *) can be computed recursively by

$$P^* = \max_{1\leq i\leq N} \delta_T(i). \tag{1}$$

$\delta_t(i)$ is defined as

$$\delta_1(i) = \pi_i b_i(o_1), \quad \forall\, 1 \leq i \leq N \tag{2}$$

$$\delta_t(j) = \max_{1\leq i\leq N} \left[\delta_{t-1}(i) a_{ij}\right] b_j(o_t), \quad \forall\, 1 \leq j \leq N, 2 \leq t \leq T, \tag{3}$$

where a_{ij} is the state transition probability from state $S_t = s_i$ to state $S_{t+1} = s_j$, $b_j(o_t)$ represents the emission probability of state $S_t = s_j$ to emit the observation o_t at time t, π_i is the initial probability of state $S_1 = s_i$ and N denotes the number of states used in the topology of the model. To decode the optimal state sequence the argument which maximized (3) must be stored in the forward step

$$\psi_1(i) = 0 \tag{4}$$

$$\psi_t(j) = \arg\max_{1\leq i\leq N} \left[\delta_{t-1}(i) a_{ij}\right], \quad \forall 1 \leq j \leq N, 2 \leq t \leq T. \tag{5}$$

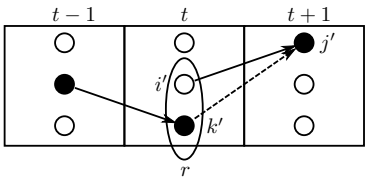

Fig. 3. Graphical illustration of the meaning of ratio r. Bold arrows indicate the state transition $a_{i'j'}$, which was chosen to maximize $\delta_{t+1}(j)$. The dashed arrow represents the transition from k' to j' skipped in this case. Black shaded circles represent states with maximum Viterbi score. The ellipsis marks the states i' and k' for which r is computed.

The optimal path is then defined by $S_t^* = \psi_{t+1}(S_{t+1}^*)$ for $t = T-1, T-2, \ldots, 1$ leading to the optimal state sequence. Accordingly, the maximum Viterbi score $\max_{1\leq j\leq N} \delta_t(j)$ at time t gives the likelihood of the optimal path of the partial observation sequence $\boldsymbol{O}_{1:t}$.

In case of defective rope regions, we assume that subsequences of the data cannot be explained well by the model. This should be reflected in the maximum Viterbi score of the according time steps, as the likelihood on the optimal path should decrease significantly. Hence, the ratio of two consecutive maximum Viterbi scores of neighboring time steps can be used as anomaly indicator and can be written as

$$R = \frac{\max_{1\leq j\leq N} \delta_{t+1}(j)}{\max_{1\leq k\leq N} \delta_t(k)} \tag{6}$$

$$= \frac{\max_{1\leq j\leq N} \max_{1\leq i\leq N} \left[\delta_t(i) a_{ij}\right] b_j(o_{t+1})}{\max_{1\leq k\leq N} \delta_t(k)} \tag{7}$$

By substituting $j' = \arg\max_{1\leq j\leq N} \delta_{t+1}(j)$, $i' = \arg\max_{1\leq i\leq N} \delta_t(i) a_{ij'}$ and $k' = \arg\max_{1\leq k\leq N} \delta_t(k)$ (7) can be rewritten as

$$R = \frac{\delta_t(i') a_{i'j'} b_{j'}(o_{t+1})}{\delta_t(k')} = \underbrace{\frac{\delta_t(i')}{\delta_t(k')}}_{r\leq 1} \underbrace{a_{i'j'} b_{j'}(o_{t+1})}_{z} \tag{8}$$

From (8) it becomes clear, that the ratio of two consecutive maximum Viterbi scores can be seen as a supplementary weightage of z given the information from the next time step. r is the ratio of the Viterbi score $\delta_t(i')$ of state i', which was chosen to maximize $\delta_{t+1}(j)$ and the maximum Viterbi score $\delta_t(k')$ in state k' at time t. This ratio can be referred to represent the structural uncertainty present in the model with respect to the input data and the optimal state at time t. The lower r becomes, the less certainty is present with regard to the choice of the optimal S_t. Fig. 3 illustrates the meaning of r. δ_{t+1} is not maximized by a transition from state $S_t = k'$ which offers the maximum $\delta_t(k)$. Instead $\delta_{t+1}(j)$

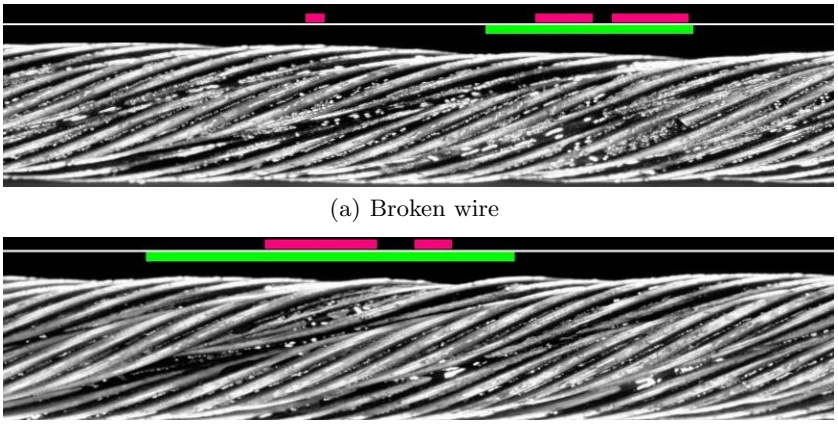

(a) Broken wire

(b) Missing wire

Fig. 4. Defect localization results on a sequence containing a broken wire (a) and a sequence with a missing wire (b). The light gray bar (green in colored version) gives the ground truth labeling of the human expert while the dark gray bar (pink in colored version) above the thin white timeline shows the obtained detection result.

becomes maximal for a transition from $S_t = s_{i'}$, although the Viterbi score $\delta_t(i')$ was not maximum. This obeys that i' was not optimal with respect to the observation sequence $\boldsymbol{O}_{1:t}$, but becomes optimal if $\boldsymbol{O}_{1:t+1}$ is considered.

As the regular characteristic of the rope implies a certain fixed structure, the structural uncertainty is supposed to grow if the underlying data cannot be explained well by the learned model. This happens if anomalies are existent in the data. A threshold on the scalar obtained by (8) for every time step t is used to evaluate the presented approach by means of ROC curves. We will call this threshold anomaly indicator in the remaining paper.

Localization results for two common rope defects are visible in Fig. 4 and clarify the potential of our theory. Although the detection results not perfectly match the ground truth labeling, regions with an anomalous visual appearance were recognized nearly to their full extent. The improvement becomes clear, if you compare the localization result for the missing wire in Fig. 4(b) with the detection result for the same defect of the same data sequence from Fig. 2. A quantitative evaluation of our approach will follow in the next section.

4 Experiments

All experiments were performed on authentic rope data acquired from real ropeways. HMM and GMM implementations of the Torch3 machine learning library [18] were employed. The number of states in the HMM was chosen to be 10 with eight components in the GMM. The HOG features were computed for blocks of 20 camera lines and a cell size of 20×20 pixels with $m = 4$ orientation bins. As

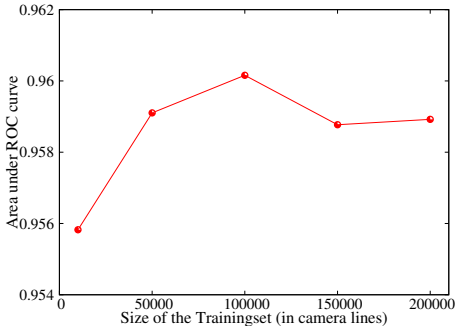

Fig. 5. Influence of the size of the training set (in camera lines) on the system performance. The performance measures are given as area under the ROC curve (AUC).

the entropy for each cell was used as additional feature, the feature dimension for a rope with 150 pixels diameter results in a size of $7 * (4 + 1) = 35$.

Model learning was done for each of the four rope views. A region which is known to be defect-free was chosen for this task. For numerical stability we used the log-likelihood instead of the likelihood, which turns the ratio in (6) into a difference. By varying the threshold on the differences of consecutive logarithmized maximum Viterbi scores, we analyzed our results with help of ROC curves. A camera line-based ratio between human-labeled defects, recovered as anomaly and the overall sum of defective camera lines was computed and is referred to as true positive rate (TPR). The false positive rate (FPR) gives a measure of the false alarm frequency. It should be noted, that the resolution of the defect location depends on the block size, used for the feature compuation.

Rope analysis was performed individually for every view given the associated model. The resulting ROC curves were averaged over all views. Interference between the views was not considered yet. Ground truth data for all experiments was given by a carefully accomplished defect labeling of a human expert.

Model learning can be done within a few minutes, as just a few rope meters are used. The time for the analysis of the rope depends on the length of the rope. In our experiments the speed for anomaly detection was approximately 6 meters per minute which leads to a processing speed up to 1000 camera lines per second (10cm/s). A parallel computation for all camera views needs approximately 3.5 hours for a rope resulting in 13.000.000 camera lines (1300 meters).

4.1 Importance of the amount of training data

The first experiment was designed to reveal the influence of the size of the training set. In Fig. 5 the area under the ROC curve (AUC) is given for different sized training sets. The ROC curves were averaged over the four rope views for a testrun on 13.000.000 camera lines (1300m of rope). Models were learned on training sets reaching from 10.000 camera lines to 200.000 camera lines (1-20m of rope). As expected, the size of the training set has an influence on the

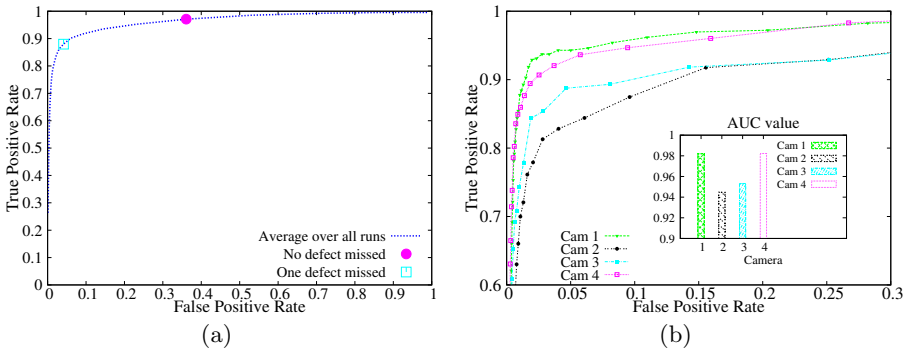

Fig. 6. Averaged ROC curve (AUC= 0.96) over all cameras and testruns (a) and ROC curves with corresponding AUC values for individual camera views (b) of a single testrun. The circle in (a) marks the recognition rates (TPR=0.97,FPR=0.36) obtained if all defects are detected while the square gives the recognition rates (TPR= 0.88, FPR= 0.04) for a tolerance range of one missed defect.

performance, because the HMM needs an adequate data basis for the estimation of the model parameters. It becomes clear, that at least 50.000 camera lines are required to obtain a robust model. In the following, experiments a training set containing 100.000 camera lines of training data was used for model learning.

4.2 Recovered Defect area

This experiment evaluates the amount of recovered defect area. The averaged result over 10 test runs with individually learned models is shown in Fig. 6(a). The AUC value for this curve is 0.96. The circle marks the first anomaly indicator value for which no defects were missed, while the square outlines the best recognition rates obtained for a tolerance range of one missed defect. The results of four individual camera views of a selected test run are visible in Fig. 6(b). It becomes clear, that cameras two and three have a weaker performance compared to one and four. This is due to missing wires which are very inconspicuous and therefore really hard to detect with an appearance based approach in these views. In Table 1 the averaged number of defects which were not discovered in the rope subjected to the value of the anomaly indicator are summarized.

Table 1. Averaged number of missed defects related to anomaly indicator value.

threshold	10	20	30	40	50	60	70	80	90
missed defects	5.925	4.750	3.675	3.100	2.275	1.100	0.000	0.000	0.000

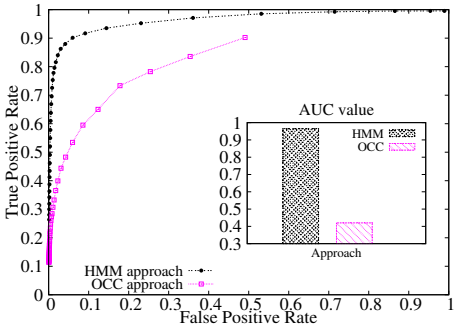

Fig. 7. Comparison of defect localization results obtained withthe OCC approach introduced in [8] and the HMM anomaly detection strategy presented in this paper.

4.3 Comparison to Time Invariant OCC

To outline the improvement concerning an automatic defect detection and localization we compare our results to the approach of Platzer et al. [8], where a time invariant OCC method was used. As in [8] the subject of interest was just a defect detection, they perform a classification postprocessing. This postprocessing step marks the whole defect area as recognized as soon as one signal window in the defect range is classified as anomaly. Hence, always 100% of the defect area is recovered unless a defect is totally missed. To compare both approaches regarding their localization ability, we skip this postprocessing for our evaluation. Fig. 7 compares the results obtained with the OCC approach and the presented HMM strategy. For both approaches, the TPR gives the percentage of recovered defect area while the FPR gives the false alarm rate. It becomes clear, that the HMM approach leads to a remarkable improvement in the defect localization compared to the OCC approach. This is a great benefit and an important aspect for the practical applicability of the system.

5 Conclusions

An new HMM-based approach for anomaly detection in wire ropes was presented. Contrary to most HMM-based anomaly detection approaches, which are based on the sequence likelihood of the whole observation sequence, a localization strategy for unusual subsequences was proposed. In contrast to the usual approaches our method needs no steering of the localization ability by choosing an effectual small signal window for the analysis. The detection of anomalous subsequences is based on the ratio of two consecutive maximum Viterbi scores. As these ratio represents a supplementary weightage of the previous chosen state transition on the optimal path, it can serve as indicator for defects in wire ropes.

Our experiments prove the working hypothesis of the paper. A context-based classification using HMMs together with our new strategy for unusual subsequence recognition can lead to an improved and more robust defect detection in

wire ropes. In experiments on real-life rope data from a ropeway it was possible to recover 90% of the overall defect area with the presented approach. At the same time, the false alarm rate stays clearly below 10%. A comparison to the work of Platzer et al. [8] in the field of visual rope inspection emphasizes the impressible improvement gained by the presented approach.

An interesting open question is still, how the dependency relations between the different rope views can be taken into account to improve the method. Furthermore, the automatic adaption of the anomaly indicator value to the data will be a point under investigation.

References

1. Mäenpää, T., Turtinen, M., Pietikäinen, M.: Real-time surface inspection by texture. Real-Time Imaging **9**(5) (2003) 289–296
2. Pernkopf, F.: 3D Surface Analysis using Coupled HMMs. Machine Vision and Applications **16**(5) (2005) 298–305
3. Xie, X., Mirmehdi, M.: TEXEMS: Texture Exemplars for Defect Detection on Random Textured Surfaces. IEEE Transactions on Pattern Analysis and Machine Intelligence **29**(8) (2007) 1454–1464
4. Xie, X.: A Review of Recent Advances in Surface Defect Detection using Texture analysis Techniques. Electronic Letters on Computer Vision and Image Analysis **7**(3) (2008) 1–22
5. Moll, D.: Innovative procedure for visual rope inspection. Lift Report **29**(3) (2003) 10–14
6. EN 12927-7: Safety requirments for cableways installations designed to carry persons. ropes. inspection, repair and maintenance. European Norm: EN 12927-7:2004 (2004)
7. Tax, D.M.J.: One-class classification - Concept-learning in the absence of counter-examples. Phd thesis, Technische Universitt Delft (2001)
8. Platzer, E.S., Denzler, J., Süße, H., Nägele, J., Wehking, K.H.: Robustness of Different Features for One-class Classification and Anomaly Detection in Wire Ropes. In: Proceedings of the 4th International Conference on Computer Vision Theory and Applications (VISAPP). Volume 1. (2009) 171–178
9. Markou, M., Singh, S.: Novelty detection: a review - part 1: statistical approaches. Signal Processing **83**(12) (2003) 2481 – 2497
10. Hodge, V., Austin, J.: A Survey of Outlier Detection Methodologies. Artificial Intelligence Review **22**(2) (2004) 85–126
11. Xie, X., Mirmehdi, M.: Localising Surface Defects in Random Colour Textures using Multiscale Texem Analysis in Image Eigenchannels. (2005) 1124–1127
12. Platzer, E.S., Denzler, J., Süße, H., Nägele, J., Wehking, K.H.: Challenging Anomaly Detection in Wire Ropes Using Linear Prediction Combined with One-class Classification. In: Proceedings of the 13th International Fall Workshop Vision, Modeling and Visualization. (2008) 343–352
13. Zhang, D., Gatica-Perez, D., Bengio, S., McCowan, I.: Semi-supervised adapted HMMs for unusual event detection. In: Proceedings of the IEEE Computer Society Conference on Computer Vision and Pattern Recognition. Volume 1. (2005) 611–618

14. Brewer, N., Nianjun, L., Vel, O.D., Caelli, T.: Using Coupled Hidden Markov Models to Model Suspect Interactions in Digital Forensic Analysis. In: International Workshop on Integrating AI and Data Mining. (2006) 58–64
15. Hadizadeh, H., Shokouhi, B.: Random Texture Defect Detection Using 1-D Hidden Markov Models Based on Local Binary Patterns. IEICE Transactions on Information and Systems **E91-D**(7) (2008) 1937–1945
16. Dalal, N., Triggs, B.: Histograms of oriented gradients for human detection. In: International Conference on Computer Vision and Pattern Recognition (CVPR). (2005) 886–893
17. Rabiner, L.R.: A Tutorial on Hidden Markov Models and Selected Applications in Speech Recognition. Proceedings of the IEEE **77**(2) (1989) 257 – 286
18. Collobert, R., Bengio, S., Mariéthoz, J.: Torch: a modular machine learning software library. Technical report, IDIAP (2002)